

Seismic Hazards in the Vicinity of Reno, Nevada

Final Technical Report

Project: 02HQGR0060

Feng Su and John G. Anderson

Seismological Laboratory
University of Nevada, Reno
Reno, Nevada 89557
Phone: (775) 784-6256
Fax: (775) 784-1833
E-mail: feng@seismo.unr.edu

August 4, 2005

Project Title: Seismic Hazards in the Vicinity of Reno, Nevada
(USGS Grant #: 02HQGR0060, 2/1/02 -1/31/05)

Under this grant, we have made important improvements on seismic hazard analysis in the Reno-Carson region. We have developed a new, comprehensive catalog of earthquakes for this area that is substantially more complete than the catalog used by the USGS 2002 hazard maps (Pancha et al, 2002, 2005). This new catalog, intended to be complete for magnitude $M > 5$, is obtained through compilation of 15 existing catalogs and supplemented by the review of 42 published journal articles. We have learned to use computer codes developed by Frankel for calculation of USGS national hazard maps. We have applied these computer codes to the probabilistic seismic hazards analysis in Reno-Carson area using geological, geodetic, and seismic history data.

We have collected GPS data from the USGS at web site <http://quake.wr.usgs.gov/research/deformation/gps/auto/CL.html>, from Kreemer and others (2000, 2003), Blewitt and others (2002), Bennett and others (2003) and Kerrmer (personal communication). Figure 1 plots the calculated hazard curves from different geodetic, geological and seismicity inputs and compares them with the hazard curve from USGS National Hazard Maps for downtown Reno. We can see the hazard curve obtained from geological faults, historical seismicity, and GPS are all very different, with the GPS data giving the highest hazard estimation. The current USGS maps use a hybrid of geological, geodetic, and seismic history data. The hazard curve from USGS National Hazard Maps is higher than the seismicity and geological estimates, but lower than that from geodesy alone. For example, at an annual occurrence rate of about 0.002/yr (1/500 yr), the USGS hazard curve shows a peak acceleration of about 0.33g, but our geodetic model predicts 0.43g, which is 30% higher than the USGS result. At an annual occurrence rate of about 0.0004/yr (1/2500 yr), the peak acceleration from the USGS model is about 0.60g, but from our geodetic model it is about 0.70g, which is about 17% higher than the USGS result (for detailed results, see attachment I).

We have conducted a productive and successful workshop on October 8, 2004, which drew over 30 geologists, geodesists, and seismologists from the regional community. By collecting presentations, information from discussions and suggestions, and searching through recent publications, we have assembled a full range of seismic hazard input information for this region. We then developed a set of improved seismic source models based on independent geodetic, geological, and seismological inputs. We have calculated probabilistic seismic hazards for each of these different models and compared these results with USGS National Seismic Hazard Map estimates (Frankel et al., 1996, Frankel et al., 2002) for this region. Following figures summarizes some of the results.

Figure 2 shows our defined study region (outlined by the box) in the Reno-Carson-Tahoe area. The orientation of the box area is chosen so that it is consistent with the regional deformation pattern. The faults distributed throughout Nevada and eastern California are those used in the USGS 2002 hazard maps calculation. Figure 3 shows our estimated

seismic moment rates from geodetic, geological and seismicity data separately in the defined region. It is very clear that the moment rate from geodetic, geological and seismological data disagree significantly. Geodetic and geological rates ought to agree, but disagreements between these and the seismicity are to be expected considering the small area and short seismic history. The differences between geodesy and geology motivate more intensive geological studies in the region. To better understand the full impact and uncertainty in seismic hazard estimates due to this difference, we conducted a multidisciplinary approach to seismic hazard analysis using independent geodetic, geological and seismicity inputs. Figure 4 to Figure 6 highlight some of the results based on the geodetic data. Figure 4 shows one of our calculated strain models based on GPS velocities. Since there are uncertainties that are associated with obtaining a strain rate model from GPS velocities, we have developed four different strain models based on additional constraints on the distribution of geodetic strain rate from geological and seismicity information. Figure 5 is the uncertainty result from these four strain models. It shows a small variance in our study region which indicates that uncertainty from strain modeling is small compared to uncertainties recognized by using other approaches. Figure 6a is the probabilistic seismic hazard map we calculated based on the strain model shown in Figure 4, compared with 2002 USGS map (Frankel et al, 2002; Figure 6b) for this area. Figures 7 and 8 highlight some of the results based on geological data. Figure 7a shows the faults with newly collected fault parameters in the region based on information from the workshop and a literature search, in comparison to the original fault database used in the USGS 2002 hazard maps calculation. We can see a significant amount of fault information, some are totally new, and some are with updated information on fault traces and slip rates have been added into our hazard map calculation. The hazard maps generated by the new fault database and the original USGS fault database are compared in Figure 8a and 8b. In general, our results indicate two important points: (1) seismic hazard estimated from geodetic input is higher in a broad area in the Reno-Carson region than the USGS national seismic hazard maps. (2) Seismic hazard estimated from fault slip rates in this region is significantly increased in the Reno and Lake Tahoe area when recent studies are included.

Resulting publications:

- Pancha, A., J.G. Anderson, and C. Kreemer (2005), Comparison of seismic and geodetic scalar moment rates across the Basin and Range province, *revision to BSSA*, June, 2005.
- Pancha, A. and John G. Anderson (2005), Basin and Range Seismicity: Distribution, occurrence rates, moment release and comparison with geodesy, Proceedings volume, Basin and Range Province Seismic Hazards Summit II, Bill Lund editor, miscellaneous publications 05-2, Utah Geological Survey.
- Su, F. and J. G. Anderson (2004). Quantifying seismic hazard uncertainty in the Reno-Carson metropolitan region, technical report on Reno-Carson Metropolitan Region Hazard Workshop, 17pp.
- Su, F., Y. Zeng and J. G. Anderson (2004). Probabilistic seismic hazards analysis using geodetic, geological and seismicity approach and its application to the Reno-Carson metropolitan region, The 3rd International Conference on Continental Earthquakes, 12-14, July, Beijing, China.

- Su, F., J. G. Anderson and A. Pancha (2005). A multidisciplinary approach to seismic hazard in the Reno-Carson metropolitan region, Proceedings of the Basin and Range Province Seismic Hazards Summit II, Bill Lund editor, miscellaneous publications 05-2, Utah Geological Survey.
- Su, F., and J. G. Anderson (2005), Quantifying seismic hazard uncertainty in the Reno-Carson metropolitan region, *SSA Annual Meeting*, Lake Tahoe.

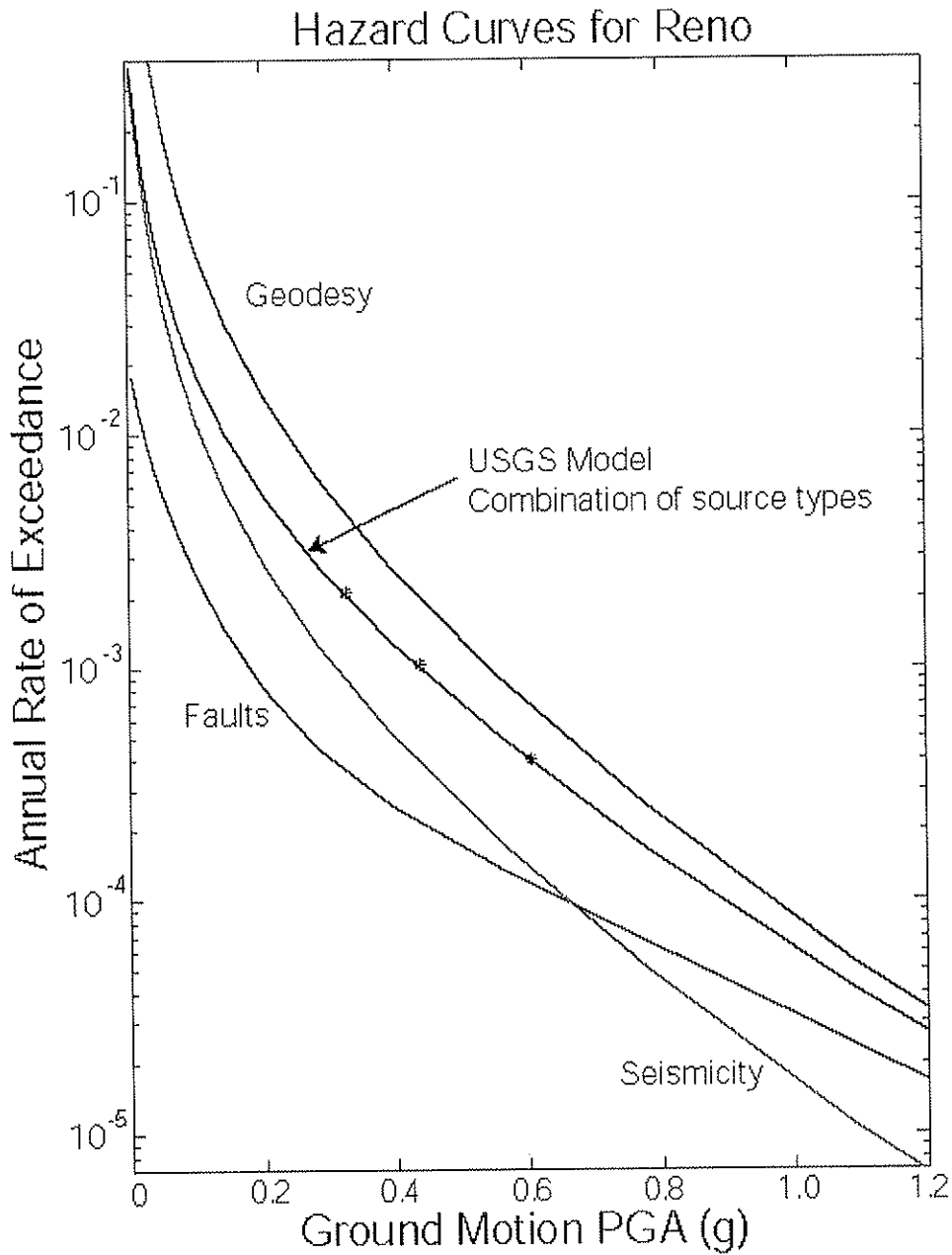


Figure 1: Plot of the seismic hazard curves we calculated in downtown Reno using different hazard models. The green line is calculated from seismicity. The black line is from faults, and blue line is from geodetic input. The red line is from USGS national hazard model.

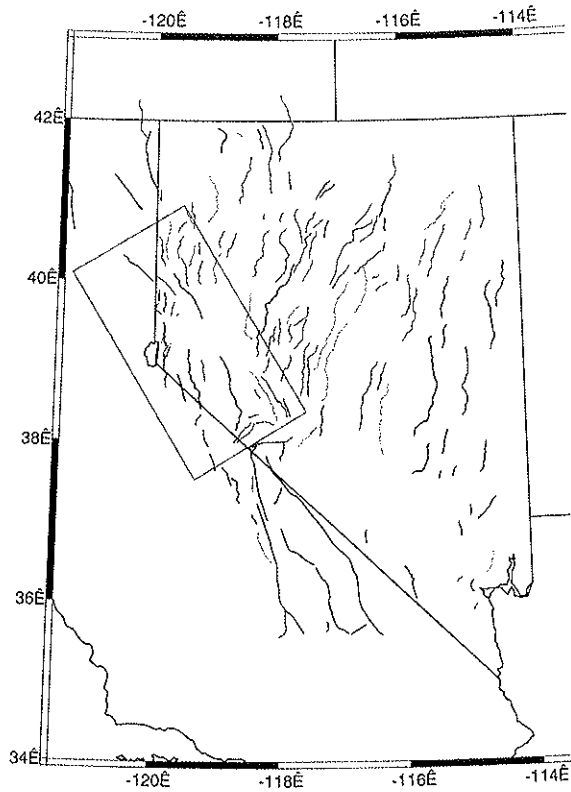


Figure 2: Map of faults in Nevada and ex used in the USGS 2002 hazard maps calcul color coded by slip rate r . Red for $r > 0.3$; $0.1 < r < 0.6$; Brown for $0.1 < r < 0.3$; Green for $r < 0.1$. The box indicate the study region.

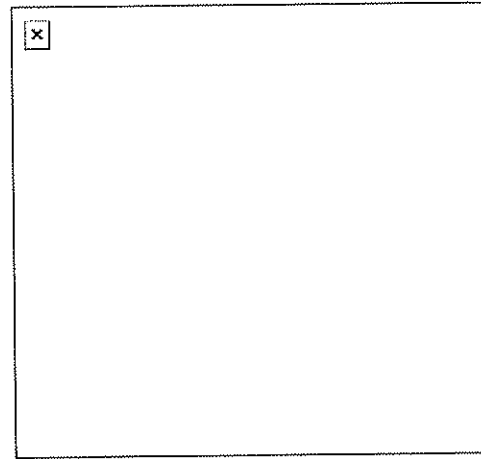


Figure 3: Comparison of seismic momer from geodetic, geological and seismicity region.

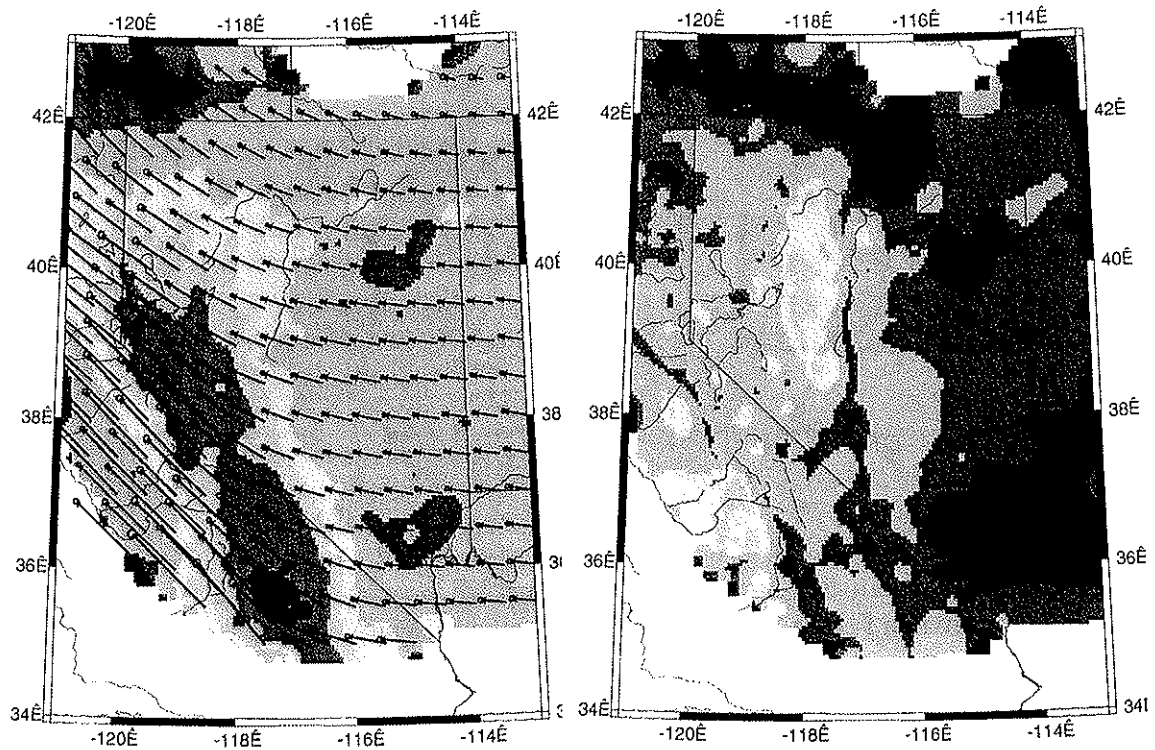
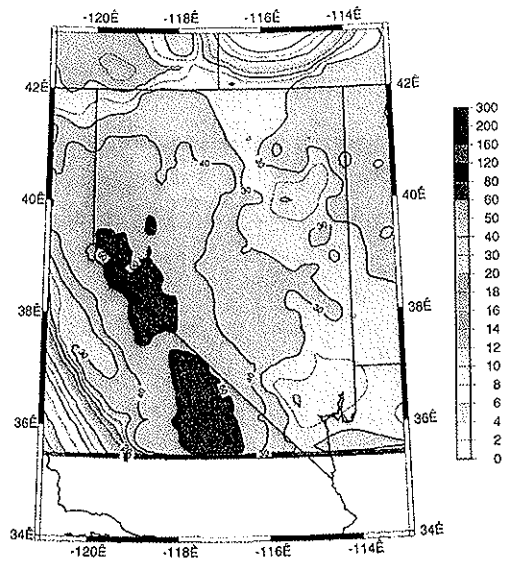
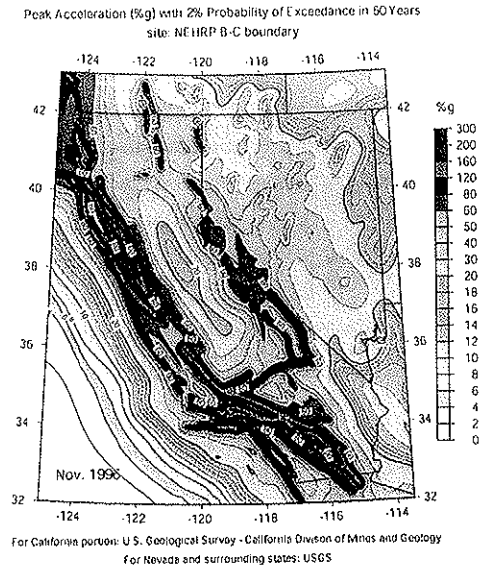


Figure 4: Contour plot of strain rate in interpolation of GPS velocities. Model's regular grid are shown as well.

Figure 5: Contour plot of the strain rate v ; four different geodetic strain rate models, e different assumptions in the data interpolati

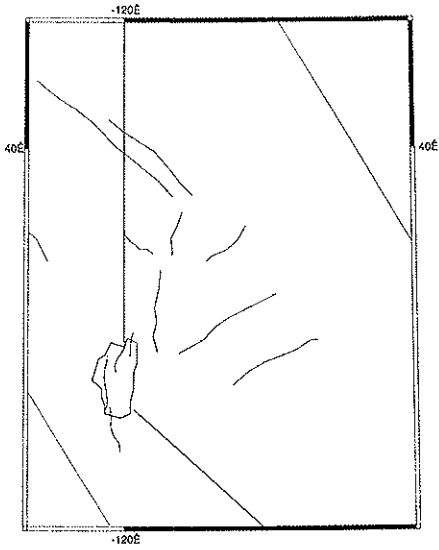


(a)

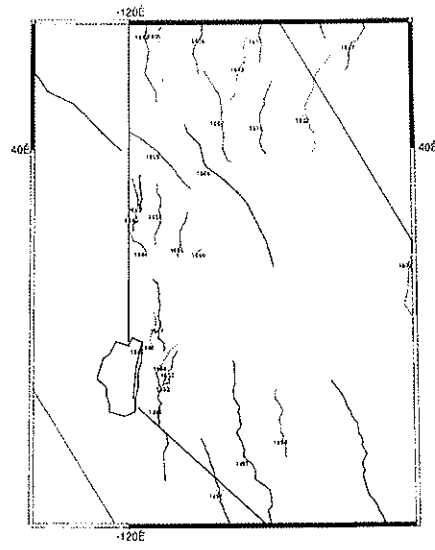


(b)

Figure 6: (a) Probabilistic seismic hazard map that we have calculated based on the strain rate model shown in Figure 5; (b) regional probabilistic seismic hazard map from USGS.



(a)



(b)

Figure 7: (a) Newly collected fault information in the study region; (b) existing faults used in the USGS 2002 hazard maps calculation.

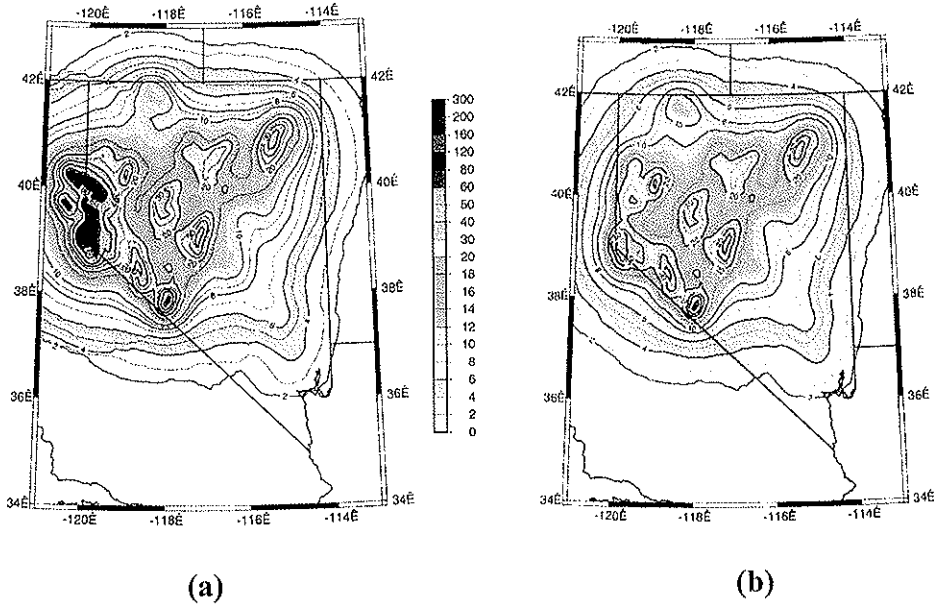


Figure 8: (a) Hazard map showing peak acceleration (% g) with 2% probability of exceedance in 50 years generated by our new fault database; (b) same as (a) but generated based on original USGS faults.

ATTACHMENT I

A Multidisciplinary Approach to Seismic Hazard in the Reno-Carson Metropolitan Region

Feng Su, John G. Anderson, and Aasha Pancha
Seismological Laboratory/ms174
University of Nevada-Reno
Reno, Nevada 89557
Phone: 775-784-4975
Fax: 775-784-4165
feng@seismo.unr.edu

ABSTRACT

In this study, we have conducted a multidisciplinary approach to seismic-hazard analysis in the Reno-Carson metropolitan region using geodetic, geological, and seismological inputs. The Reno-Carson region is the second most populous area in Nevada and lies in one of the most seismically active parts of the state. Rates of deformation in the region have very large uncertainties. Currently available geodetic, geological, and seismological data disagree significantly. To investigate the impact and uncertainty in hazard estimates resulting from these differences, we have developed a set of seismic source models based on independent geodetic, geological, and seismological inputs and calculated probabilistic seismic hazards for each of these models. We then compare these results with USGS National Seismic Hazard Map estimates (1996, 2002) for this region. Our results indicate that geodetic input predicts the highest hazard. For example, in downtown Reno at an annual occurrence rate of about 0.002/yr (1/500 yr), the USGS hazard curve shows a peak acceleration of about 0.33g, but our geodetic model predicts 0.43g, which is 30% higher than the USGS result.

INTRODUCTION

The Reno-Carson metropolitan area is the second most populated region in Nevada. It lies in one of the most seismically active parts of the state. Thirteen earthquakes of magnitude 6 or greater have occurred in the region since 1850 (dePolo and others, 1997). While the region has been seismically active in historic time, recent seismicity has been low. The study region lies within the Basin and Range Province, which extends from the rigid Sierra Nevada block in the west to the Colorado Plateau in the east. Geodetic measurements show concentrated deformation at the eastern and western edges of the Basin and Range, with little deformation in between (Thatcher *and others*, 1999). Part (about 25%) of the Pacific-North American relative plate motion is taken up by displacement and deformation in the Basin and Range Province. Along the western edge of the Basin and Range, geodesy shows a widening of the deformation zone from south to north (Figure 1). Motion west of about 118°W is approximately parallel to the Pacific Plate motion vector (Thatcher, 1999; Bennett *and others*, 2003; Hammond and Thatcher, 2004), suggesting coupling of the plate motion. The Sierra Nevada behaves as a block, and moves northwest at about 13 mm/yr. Motions east of the Sierra Nevada Range between 118° W and 120° W are approximately parallel to the motion of the Sierras (Thatcher *and others*, 1999). Relative motion, oriented N37°W ± 2°W, between the Sierra Nevada Great Valley and central Great Basin regions occurs at a rate of 9.3 ± 0.2 mm/yr (Bennett *and others*, 2003). The greatest deformation takes place across a zone of conjugate strike-slip and normal faults, at a rate of 12.5 ± 0.15 mm/year between 119.1°W and 120.2°W. More recent data confirm this observation, with velocities west of 117.7°W increasing from ~1 mm/yr to ~12 mm/yr (Bennett *and others*, 2003; Hammond and Thatcher, 2004). This high velocity gradient implies high seismic risk, and increases the potential for more frequent damaging earthquakes. Other recent publications, such as Dixon and others (2000), Wernicke and others (2000), Cashman and Fontaine (2000), dePolo and others (2001), Svarc and others (2002), Oldow (2003), and Unruh and others (2003) also provide insight on deformation rates in the region. Geological slip rates are not well known for the study region, with many faults uncharacterized. The inferences from geodetic data suggest the greatest deformation rates compared to those from either seismicity or geology.

In this study, we have conducted a multidisciplinary approach to seismic-hazard analysis in the area using independent geodetic, geological, and seismological inputs. By comparing results from this wide range of independent models, we hope to better understand the uncertainties and the consequences of these uncertainties for the probabilistic seismic hazard of the area.

METHOD

According to Gutenberg-Richter's frequency-magnitude relation, the number of seismic events with magnitude between $M-dM/2$ and $M+dM/2$ is given by $n(M)dM$, where $n(M)=10^{a-bM}$.

The moment rate \dot{M}_0 is related to the earthquake-occurrence rate by

$$M_0^{\&} = \int_{\infty}^{\infty} M_0 n(M) dM = \int_{\infty}^{\infty} M_0 10^{a-bM} dM \quad (1)$$

Using the moment-magnitude relation

$$M_0 = 10^{1.5M+c} \quad (2)$$

where c is a constant. This study uses $c=16.095$ (cgs units) as defined by Hanks and Kanamori (1978).

Substitute (2) into (1), we obtain

$$\begin{aligned} M_0^{\&} &= \int_{\infty}^{\infty} 10^{1.5M+c+a-bM} dM = \int_{\infty}^{\infty} 10^{a+c+(1.5-b)M} dM \\ &= \frac{10^{a+c}}{(1.5-b)\ln 10} 10^{(1.5-b)M} \Big|_{M_{\min}}^{M_{\max}} \end{aligned} \quad (3)$$

For $b < 1.5$

$$M_0^{\&} \approx \frac{10^{a+c+(1.5-b)M_{\max}}}{(1.5-b)\ln 10} \quad (4)$$

Equation (4) is the same as the result from Anderson (1979).

According to Ward (1994, 1998a, b) the minimum geodetic moment rate in a region can be estimated using the maximum eigenvalue of a 2-D strain-rate tensor, i.e., the principle surficial extension and contraction rates:

$$M_0^{\&} = 2\mu A H_s \text{Max}(|\&_x|, |\&_y|) \quad (5)$$

where $\&_x$ and $\&_y$ are the principle surficial extension and contraction rates, A is the surface area and H_s is the seismogenic thickness of the region.

Assuming the b value and the maximum magnitude M_{\max} for the region, we can then estimate the a value for a given seismic-moment-rate distribution. The result is given by

$$10^a = M_0^{\&} (1.5-b) \ln 10 / 10^{c+(1.5-b)M_{\max}} \quad (6)$$

ANALYSIS AND RESULTS

Figure 2 shows the distribution of faults in Nevada and eastern California, with faults color coded by activity rate. These faults are used in the calculation of the USGS 2002 National Hazard Maps. Our focus area is outlined by the box. The orientation of the box is chosen so that it is consistent with the orientation of stresses in the region. From the figure we can see this area contains some of the most active faults of the state, as shown by their color.

For the geodetic data, we have collected GPS data from the USGS at web site <http://quake.wr.usgs.gov/research/deformation/gps/auto/CL.html>, from Kreemer and others (2000, 2003), Blewitt and others (2002), Bennett and others (2003), and Blewitt and Coolbaugh (personal communication). In a recent work, Blewitt and others (2002) built a geodetic velocity database containing GPS, Satellite Laser Ranging and Very Long Baseline Interferometry data obtained across the Basin and Range from more than 42 studies. We have used their inverted strain-rate field data to obtain a geodetic-moment rate using Ward's approach (Equation 5). To compute probabilistic seismic hazard maps using geological and historical seismicity models, we have followed the method used by USGS in their National Seismic Hazard Map generation.

Figure 3 plots the calculated hazard curves from each of these different hazard models and compares them with the hazard curve from USGS National Hazard Maps for downtown Reno. We can see the hazard curve obtained from geology faults, historical seismicity, and GPS are all very different, with the GPS data giving the highest hazard estimation.

The current USGS maps use a hybrid of geological, geodetic, and seismic history data. The hazard curve from USGS National Hazard Maps is higher than the seismicity and geological estimates, but lower than that from geodesy alone. For example, at an annual occurrence rate of about 0.002/yr (1/500 yr), the USGS hazard curve shows a peak acceleration of about 0.33g, but our geodetic model predicts 0.43g, which is 30% higher than the USGS result. At an annual occurrence rate of about 0.0004/yr (1/2500 yr), the peak acceleration from the USGS model is about 0.60g, but from our geodetic model it is about 0.70g, which is about 17% higher than the USGS result.

We have also calculated the moment rate in this region based on geodetic, geological, and seismicity inputs. The moment rate is about 0.83×10^{25} dyne-cm/yr from seismicity and about 0.37×10^{25} dyne-cm/yr from faults. Since our region is about 334 km long, this is equivalent to a through-going, strike-slip fault with a displacement rate of 2 mm/yr. The moment rate calculated based on maximum shear strain in this region is about 2.7×10^{25} dyne-cm/yr. So, according to GPS data, the relative shear in the region is much greater. We take this as an indication that so far, the geological mapping is not sufficiently complete to associate all of the plate motion with faults.

DISCUSSION AND CONCLUSION

A challenge facing seismic-hazard assessment in the Reno-Carson area is the inconsistency among the seismic-moment rates estimated using geodetic, geological, and historical seismicity data. This inconsistency may be due to the lack of information regarding historical seismicity and paleoseismic data in this area. Under this hypothesis, GPS data has the advantage in that it can provide information on deformation within the network even if that activity occurs on faults that are unknown, too slowly slipping, or too deep to study by traditional methods. On the other hand, there are questions regarding how much the GPS data might be affected by transient behavior that follows past large earthquakes. Since geodesy, geology, and historical seismicity each provide a different view of the regional deformation, inconsistencies or consistencies among the results from

different approaches will reveal new insights into the seismic hazard of this region. Based on present geodetic data, current seismic hazard for Reno may be underestimated.

The curves shown in Figure 3 present a preliminary result. Further studies will involve sensitivity tests. For instance, for the GPS data, there is the non-uniqueness and uncertainty involved with converting surface strain to a scalar-moment rate. Currently, there are several techniques for this in the literature. We have followed Ward's approach, which provides a minimum estimate of the geodetic-moment rate in the region. In addition, we have used an underdamped version of the geodetic strain field. Further understanding of the geodetic data is required to identify where strain may be poorly predicted due to lack of station coverage.

ACKNOWLEDGMENTS

We thank Dr. David Von Seggern and Bill Lund for their careful review and valuable comments. This work is supported by USGS grant 02HQGR0060.

REFERENCES

- Anderson, J. G., 1979, Estimating the seismicity from geological structure for seismic-risk studies, *Bull. Seism. Soc. Am.*, 69, 135-158.
- Bennett, RA, Wernicke, BP, Niemi, NA, Friedrich, AM, Davis, JL, 2003, Contemporary strain rates in the northern Basin and Range province from GPS data, *Tectonics* 22, Is 2, Article 1008, 31 pg.
- Blewitt, G., Coolbaugh, M., Holt, W., Kreemer, C., Davis, J. and Bennett, R., 2002, Targeting of potential geothermal resources in the Great Basin from regional relationships between geodetic strain and geological structures, *Transactions Geothermal Resources Council*, Vol. 26, p. 523-526.
- Cashman, P. H. and Fontaine, S. A., 2000, Strain partitioning in the northern Walker Lane, western Nevada and northeastern California, *Tectonophysics* 326, 111-130.
- dePolo, C. M., J. G. Anderson, D. M. dePolo, and J. G. Price (1997). Earthquake occurrence in the Reno-Carson city urban Corridor, *Seismological Research Letters*, 68, p. 401-412.
- dePolo, C. M., A. R. Ramelli, R. H. Hess and J. G. Anderson, 2001, Reevaluation of pre-1900 earthquakes in western Nevada, Final Technical Report to NEHRP, Grant 99HQGR0083, Nevada Bureau of Mines and Geology, University of Nevada, Reno.
- Dixon, T. H., Miller, M., Farina, F., Wang, H., Johnson, D., (2000). Present-day motion of the Sierra Nevada block and some tectonic implications for the Basin and Range Province, North American Cordillera, *Tectonics*, vol.19, no.1, pp.1-24, Feb 2000.
- Hammond, W. C., and W. Thatcher (2004), Contemporary tectonic deformation of the Basin and Range province, western United States: 10 years of observation with the Global Positioning System, *J. Geophys. Res.*, in press.
- Hanks, T. C., and H. Kanamori, 1978, A Moment Magnitude Scale, *J. Geophys. Res.*, 84, 2348-2350.
- Kreemer, C., Haines, J., Holt, W. E., Blewitt, G. and D. Lavallee, 2000, On the determination of a global strain rate model, *Earth, Planets Space*, 52, 765-770.

Kreemer, C., Holt, W. E. and J. Haines, 2003, An integrated global model of present-day plate motions and plate boundary deformation, *Geophys. J. Int.*, 154, 8-34.

Oldow, JS, (2003). Active transtensional boundary zone between the western Great Basin and Sierra Nevada block, western US cordillera, *Geology* 31, 1033-1036.

Svarc, JL; Savage, JC; Prescott, WH; Ramelli, AR., 2002, Strain accumulation and rotation in western Nevada, 1993-2000. *Journal Of Geophysical Research-Solid Earth* 107 (B5): art. no.-2090.

Thatcher, W., G. R. Foulger, B. R. Julian, J. Svarc, E Quilty and G. W. Bawden (1999). Present day deformation across the Basin and Range province, western United States, *Science* 283, 1714-1718.

Unruh, J, Humphrey, J, Barron, A (2003). Transtensional model for the Sierra Nevada frontal fault system, eastern California, *Geology* 31, 327-330.

Ward, S. N. (1994). A multidisciplinary approach to seismic hazard in Southern California, *Bull. Seism. Soc. Am.*, 84, 1293-1309.

Ward, S. N. (1998a). On the consistency of earthquake moment rates, geological fault data, and space geodetic strain: the United States, *Geophys. J. Int.*, 134, 172-186.

Ward, S. N. (1998b). On the consistency of earthquake moment rates, geological fault data, and space geodetic strain: Europe, *Geophys. J. Int.*, 135, 1011-1018.

Wernicke, B., A. Friedrich, N. A. Neimi, R. A. Bennett, J. L. Davis (2000). Dynamics of plate boundary fault systems from Basin and Range geodetic network (BARGEN) and geologic data, *GSA Today*, 10, No. 11, Nov. 2000, 1-7.

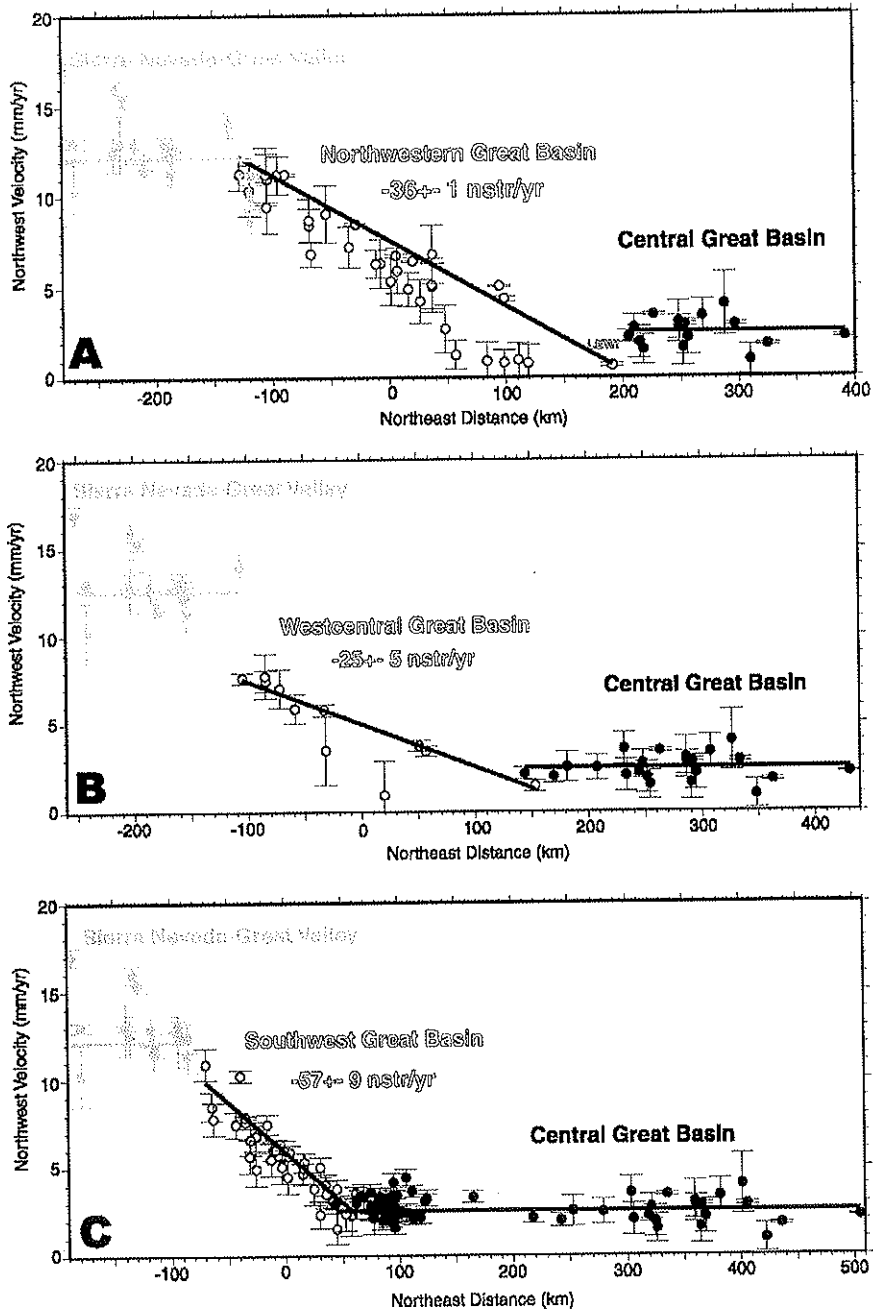


Figure 1: Reproduced from Figure 14 of Bennett and others (2003). (a) $N37^{\circ}W$ components of velocity as a function of $N53^{\circ}E$ distance for the Sierra Nevada Great Valley (gray circles), northwestern Great Basin (open circles), and central Great Basin (solid circles) domains. Velocities refer to the North America reference frame. Error bars represent 1 standard deviation. The lines show the block-strain model. Zero slopes indicate the region is not internally deforming. (b) Same as for figure 1a but for west central Great Basin domain. (c) Same as for figure 1a but for southwestern Great Basin domain.

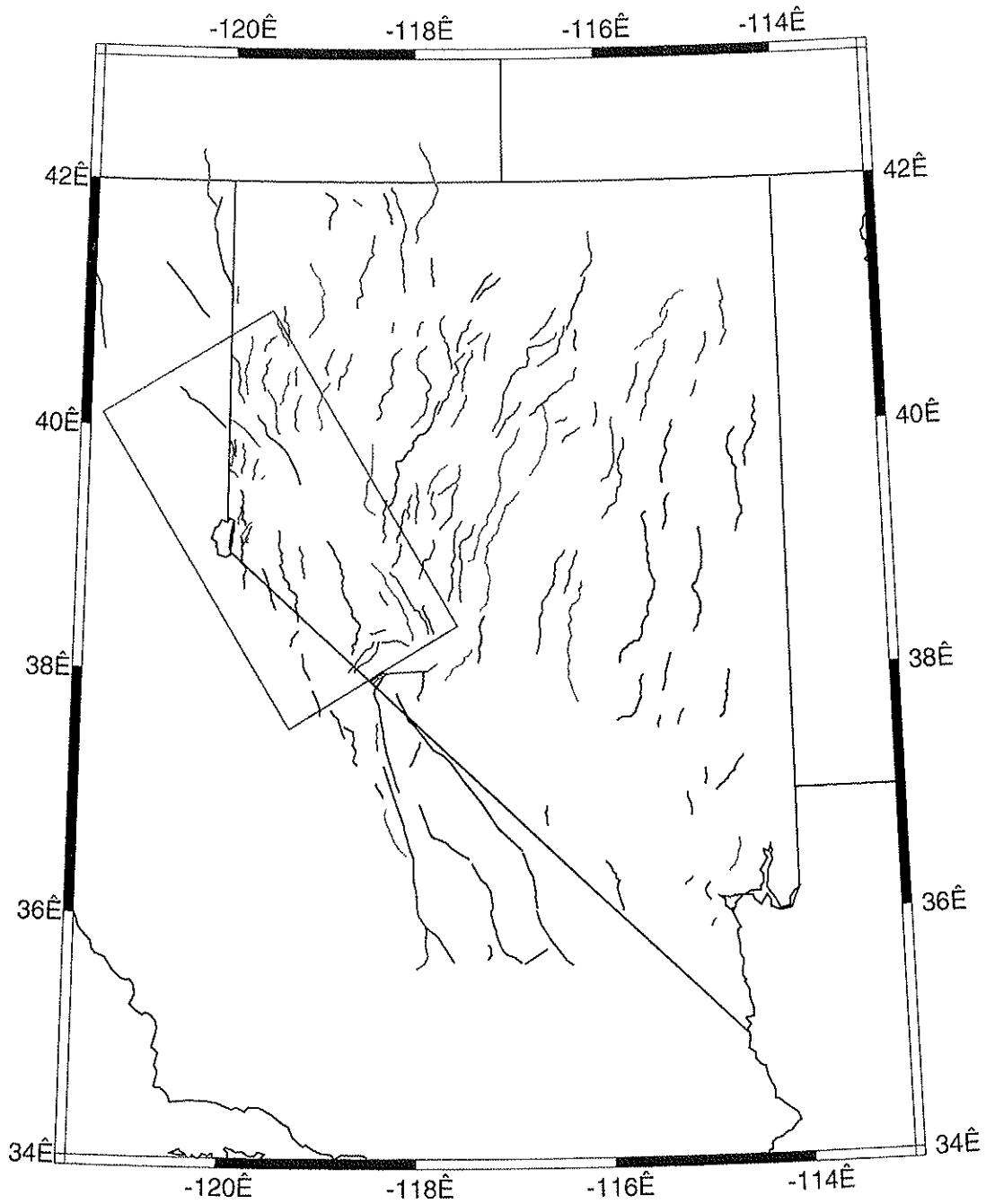


Figure 2: Map of faults in Nevada and eastern California used in the USGS 2002 hazard maps calculation. Faults are color coded by slip rate r . Red for $r > 0.6$ mm/yr, Purple for $0.3 < r < 0.6$ mm/yr; Brown for $0.1 < r < 0.3$ mm/yr; Green for $r = 0.1$ mm/yr and Blue for $r < 0.1$ mm/yr. The box indicates our study region.

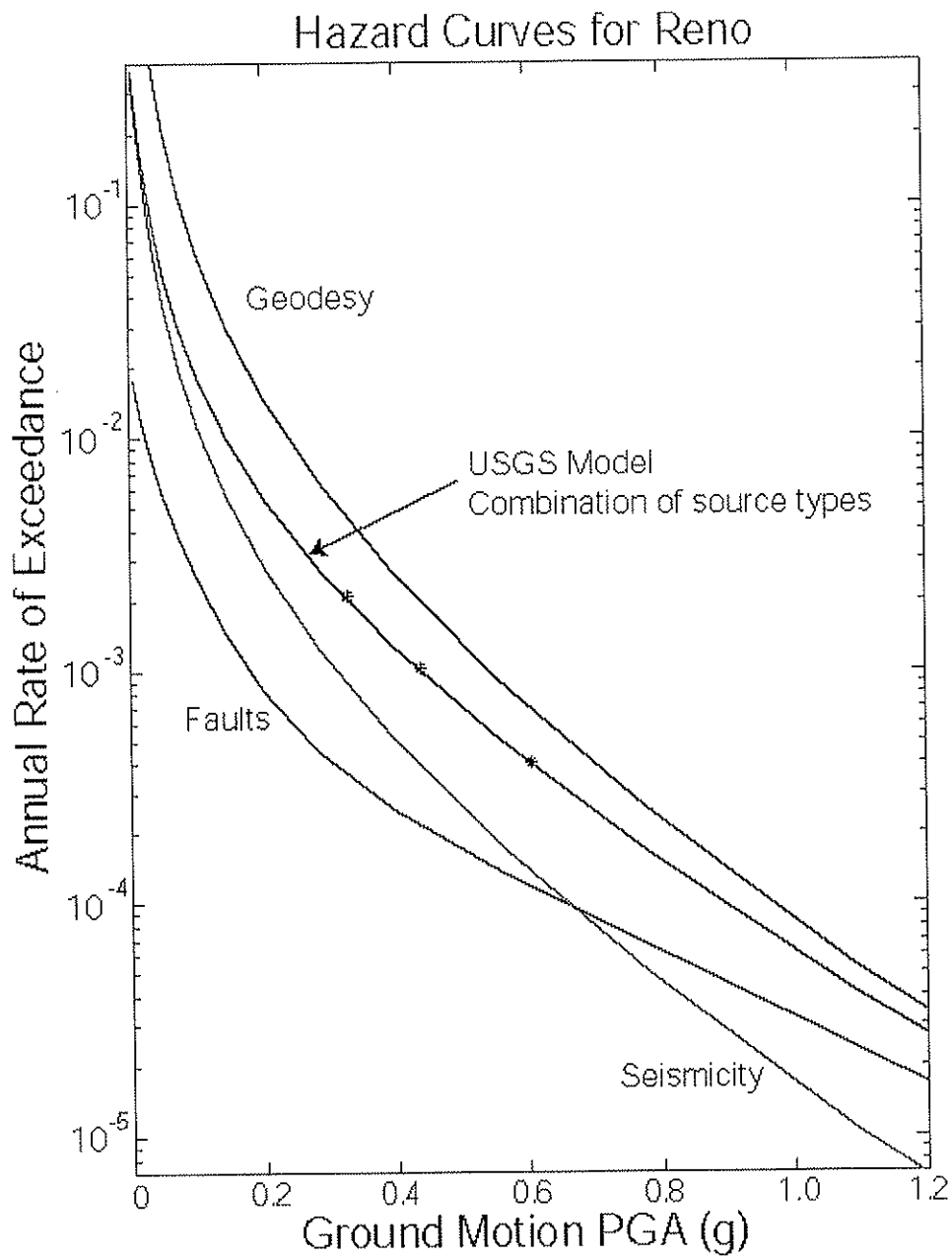


Figure 3: Plot of the seismic hazard curves we calculated in downtown Reno using different hazard models. The green line is calculated from seismicity. The black line is from faults, and blue line is from geodetic input. The red line is from USGS national hazard model.

